


Research Article

Antioxidant and Antibacterial Activities of Silver Nanoparticles Biosynthesized by *Moringa oleifera* through Response Surface Methodology

A. B. Abeer Mohammed,¹ Amr Mohamed,¹ Noura El-Ahmady El-Naggar ²,
Hoda Mahrous,³ Ghada M. Nasr,⁴ Asmaa Abdella,³ Rasha H. Ahmed ⁵, Sibel Irmak,⁶
Mohamed S. A. Elsayed,⁷ Samy Selim ⁸, Amr Elkelish ⁹, Dalal Hussien M. Alkhalifah,¹⁰
Wael N. Hozzein ¹¹ and Abdallah S. Ali ⁵

¹Department of Microbial Biotechnology, Genetic Engineering and Biotechnology Research Institute, University of Sadat City, Egypt

²Department of Bioprocess Development, Genetic Engineering and Biotechnology Research Institute, City of Scientific Research and Technological Applications (SRTA-City), New Borg El Arab City, 21934 Alexandria, Egypt

³Department of Industrial Biotechnology, Genetic Engineering and Biotechnology Research Institute, University of Sadat City, Egypt

⁴Department of Molecular Diagnostics, Genetic Engineering and Biotechnology Research Institute, University of Sadat City, Egypt

⁵Department of Microbiology, Faculty of Agriculture, Cairo University, 12613 Giza, Egypt

⁶Department of Agricultural and Biological Engineering, Pennsylvania State University, University Park, PA 16802, USA

⁷Department of Bacteriology, Mycology, and Immunology, Faculty of Veterinary Medicine, University of Sadat City, Menoufia 32897, Egypt

⁸Department of Clinical Laboratory Sciences, College of Applied Medical Sciences, Jouf University, Sakaka, 72388, Saudi Arabia

⁹Botany Department, Faculty of Science, Suez Canal University, Ismailia, Egypt

¹⁰Department of Biology, College of Science, Princess Nourah Bint Abdulrahman University, P.O. Box 84428, Riyadh 11671, Saudi Arabia

¹¹Botany and Microbiology Department, Faculty of Science, Beni-Suef University, Beni-Suef, Egypt

Correspondence should be addressed to Rasha H. Ahmed; rasha.hussien@agr.cu.edu.eg

Received 12 January 2022; Accepted 21 March 2022; Published 20 April 2022

Academic Editor: José Agustín Tapia Hernández

Copyright © 2022 A. B. Abeer Mohammed et al. This is an open access article distributed under the Creative Commons Attribution License, which permits unrestricted use, distribution, and reproduction in any medium, provided the original work is properly cited.

The research highlights the environmentally sustainable biosynthesis of silver nanoparticles from fresh leaves of the herbal medicinal plant *Moringa oleifera*. They may have been used as anti-inflammatory, anticancer, and antimicrobial agents. *M. oleifera* extract both reduces and stabilizes silver nanoparticles (AgNPs). Optimum factors needed for AgNP biosynthesis were studied using a central composite design (CCD) matrix. Ultraviolet-visible (UV-Vis) absorption spectroscopy, transmission electron microscopy, and Fourier-transform infrared spectroscopy were used to confirm and characterize the synthesized AgNPs. The biogenic AgNPs demonstrated substantial antibacterial potential against the pathogenic strains *Escherichia coli*, *Klebsiella pneumoniae*, *Staphylococcus aureus*, and *Bacillus subtilis*. The antioxidant activity of biosynthesized AgNPs with *M. oleifera* extract increased from 11.96% when the concentration of the extract was 4 mg/mL to 63.79% at a plant concentration of 20 mg/mL. This research provides an easy and cost-effective technique for the production of stable nanoparticles, with an evaluation of their bioactivity.

1. Introduction

Nanoparticles (NPs) can be generated by various chemical, biological, and physical methods [1, 2]. Biological approaches are preferred because they are environmentally friendly [3], competitive [4], and more economical than other approaches [5]. NPs can be created using microorganisms or medicinal plants [6]. Green synthesis is performed by environmentally friendly materials such as herbs and bacteria for NP biosynthesis [7]. This increases the therapeutic value of the NPs produced because the plant phytochemicals provide antioxidant and antibacterial activities for the synthesized silver nanoparticles (AgNPs) [8]. The potential uses of plant materials in the green synthesis of NPs eliminate the need for additional procedures, such as intracellular purification steps for the synthesized compounds and the cultivation of microbial cell cultures [9].

Silver has long been recognized as an antimicrobial agent, and AgNPs are nontoxic to eukaryotes such as humans; despite this, AgNPs are extremely poisonous to prokaryotic cells such as bacteria [10]. Researchers are studying their applications in nanomedicine because of their antimicrobial [11], antiplatelet [12], anticancer [13], and wound healing properties [14]. The high surface area-to-volume ratios of AgNPs ensure high reactivity in biomedical research [15]. Various studies have been documented on plant extracts used for AgNP synthesis, such as *Papaver somniferum* [16], *Bauhinia variegata* L. [17], *Hevea brasiliensis* [18], *Aloe vera* [19], and *Acacia farnesiana* [20]. In these studies, phytochemical extracts were used as alternative precursors for reducing or capping the silver from silver nitrate during the biosynthesis of AgNPs [16].

Moringa oleifera is widely disseminated and used throughout the world's tropical and subtropical regions, and it is native to India and Africa [21]. It has been used for centuries because of its health benefits and medicinal properties. *M. oleifera* leaves contain a variety of beneficial chemicals. These are classified into carotenoids, vitamins, glucosinolates, polyphenols, flavonoids, phenolic acids, oxalates, isothiocyanates, alkaloids, phytates, saponins, and tannins [22]. The medicinal significance of *M. oleifera* is associated with its high antioxidant activity, as well as its substantial antibacterial activity [23]. *M. oleifera* has been reported to synthesize natural bioactive compounds such as flavonoids and terpenoids. These compounds have been discovered to be potential antimicrobials against pathogenic microorganisms [24–27]. Various studies have documented the biosynthesis of AgNPs from *M. oleifera* and assessed their many potential uses, such as antimicrobial agents [27–35], their sensing properties [27], water detoxification abilities [31], and their anticancer potential [33].

In the current study, *M. oleifera* was used as a low-cost and environmentally acceptable precursor for bioreduction, biostabilization, and biocapping of silver in the biosynthesis of AgNPs with antibacterial activity. Green chemistry principles were designed for the biosynthesis of AgNPs. The biosynthesis parameters were optimized using a central composite design (CCD) with response surface methodology. The antibacterial and antioxidant activities of bio-

synthesized AgNPs were assessed against the pathogenic human bacteria *Escherichia coli*, *Klebsiella pneumoniae*, *Staphylococcus aureus*, and *Bacillus subtilis*.

2. Results and Discussion

2.1. Evaluation of AgNP Biosynthesis Using *M. oleifera* Leaf Extract and UV-Visible Spectral Analysis. Silver nanoparticles were biosynthesized using an extract of *M. oleifera* leaves mixed with 50 mL when added to an aqueous solution of silver nitrate (1 mM). The reaction mixture was maintained in complete darkness. The color changed from pale brown to dark brown, indicating that AgNPs were formed. A dark brown coloration of the solution following the reaction with the Ag⁺ ions is an obvious indicator of metal ion reduction and the formation of AgNPs. Due to the excitation of silver nanoparticles' surface plasmon vibrations, AgNPs exhibit a light yellow to brown coloration [36]. The authors in many previous studies apply a variety of AgNO₃ concentrations, varying from 0.1 mM to 1 M, in the biosynthesis of AgNPs. For the biosynthesis of AgNPs, the most frequently used concentration of AgNO₃ is 1 mM when an aqueous extract of *Plectranthus amboinicus* leaves is used [37]. Sadeghi and Gholamhoseinpoor [38] synthesized AgNPs from a methanol-extracted aqueous filtrate of *Ziziphora tenuior* leaves using 0.1 mM AgNO₃. On the other contrary, AgNP production required 500 mM of AgNO₃ mixed with a vacuolevaporated methanol extract of *Viburnum lantana* leaves [39], while Veerasamy et al. [40] employed 5 mM of AgNO₃ in the synthesis of AgNPs using aqueous filtrate of *Garcinia mangostana* leaves as a reducing agent.

Scanning UV-visible spectroscopy in the 200–800 nm region was used to confirm the biosynthesis of AgNPs. The surface plasmon resonance (SPR) spectroscopy of silver nanoparticles synthesized using extract *Moringa oleifera* leaves confirmed the presence of AgNPs via a prominent absorption band at 460 nm. This result was consistent with Sarkar et al.'s [41] finding. The absorption spectrum of SPR is greatly influenced by stabilizing molecules, particle size, and particles adsorbing to the surface. When the size of silver nanoparticles in aqueous solution increases, the SPR peak changes to longer wavelengths [42].

2.2. Biosynthesis Optimization of AgNPs. The RSM is a strategy that is based on the fundamental concepts of statistics as well as random assignment and validation. It is a highly successful statistical strategy that contributes to the simplification of the optimization of a large number of variables in order to anticipate the optimal processing conditions with the fewest possible experiments and to explain the individual and the mutual interactions of independent variables throughout a range of possible values on the response [43]. Table 1 displays the experimental results of the CCD matrix of the main variables, as well as related biosynthesized AgNPs ($\mu\text{g/mL}$). The CCD experiments showed a large variance in AgNP biosynthesis; this variance reflected the importance of the optimization process in AgNP biosynthesis. There was a broad variation in AgNP biosynthesis ranging from 0.227 to 3.068 $\mu\text{g/mL}$ across the various CCD trials.

TABLE 1: The experimental and predicted values of silver nanoparticle biosynthesis with *Moringa oleifera* leaf extract were designed by central composite design.

Run	Initial pH level (X_1)		Temperature (X_2)		Incubation time (X_3)		Plant extract volume (X_4)		AgNPs ($\mu\text{g/mL}$)	
	Coded	Actual	Coded	Actual ($^{\circ}\text{C}$)	Coded	Actual (hr)	Coded	Actual (mL)	Experimental	Predicted
1	1	10	1	80	-1	6	-1	1	2.004	1.980
2	-1	6	1	80	1	10	-1	1	1.069	1.083
3	0	8	0	60	0	8	0	1.5	1.49	1.350
4	1	10	1	80	1	10	1	2	2.088	2.043
5	0	8	0	60	0	8	0	1.5	1.249	1.350
6	0	8	0	60	0	8	-2	0.5	1.973	2.047
7	-1	6	-1	40	-1	6	1	2	0.603	0.808
8	0	8	0	60	2	12	0	1.5	2.002	2.032
9	0	8	-2	20	0	8	0	1.5	0.772	0.817
10	1	10	-1	40	-1	6	1	2	1.964	1.761
11	0	8	0	60	0	8	0	1.5	1.318	1.350
12	-2	4	0	60	0	8	0	1.5	0.227	0.117
13	-1	6	-1	40	1	10	1	2	1.0591	0.894
14	1	10	-1	40	-1	6	-1	1	1.272	1.278
15	1	10	-1	40	1	10	-1	1	2.969	2.819
16	0	8	0	60	-2	4	0	1.5	0.903	0.993
17	0	8	2	100	0	8	0	1.5	0.852	0.927
18	2	12	0	60	0	8	0	1.5	2.69	2.920
19	0	8	0	60	0	8	2	2.5	1.704	1.749
20	-1	6	-1	40	-1	6	-1	1	0.361	0.217
21	-1	6	1	80	-1	6	1	2	0.842	0.804
22	1	10	-1	40	1	10	1	2	2.646	2.718
23	-1	6	-1	40	1	10	-1	1	0.719	0.887
24	1	10	1	80	1	10	-1	1	3.068	2.932
25	0	8	0	60	0	8	0	1.5	1.305	1.350
26	0	8	0	60	0	8	0	1.5	1.245	1.350
27	0	8	0	60	0	8	0	1.5	1.492	1.350
28	-1	6	1	80	-1	6	-1	1	1.004	1.001
29	-1	6	1	80	1	10	1	2	0.24	0.302
30	1	10	1	80	-1	6	1	2	1.775	1.675

The difference underlined the significance of the optimization process in achieving a higher biosynthesis of AgNPs. Table 2 shows the results of the statistical analysis using multiple regression and variance analysis (ANOVA) for CCD results of AgNP biosynthesis using *M. oleifera* leaf extract.

The coefficients' signs (positive or negative effect on the response) and statistical significance were used to interpret the data. Interactions between two variables can be antagonistic (negative coefficient) or synergistic (positive coefficient) (positive coefficient) [44]. The estimated coefficients with negative values (Table 2) imply an antagonistic relationship between variables and the biosynthesis of AgNPs, while positive coefficients imply a synergistic interaction between variables and the biosynthesis of AgNPs. If the value is close to zero, it indicates that the process variable has low to no influence on AgNP biosynthesis. The contri-

bution percentages for the various variables are shown in Table 2.

To determine the significance of each coefficient, P values were used. This is necessary for understanding the behavior of independent variables and their mutual interactions [36]. The factors with a confidence level greater than 95% (.) were considered significant. Thus, the process factors with $P < 0.05$ and confidence level > 95 percent) were judged to have a significant effect on silver nanoparticle production [45]. The most important factors influencing AgNP biosynthesis were pH ($P < 0.0001$), time of incubation ($P < 0.0001$), and plant extract volume ($P = 0.0361$). The quadratic effects of the temperature and the plant extract volume were also found to be significant with P values of 0.0013 and 0.0004, respectively. It was also noticed that the interaction effects between pH \times incubation time, temperature \times incubation time, temperature \times the plant

TABLE 2: ANOVA and regression coefficients for CCD results of AgNP biosynthesis using *M. oleifera* leaf extract.

Source of variance		Sum of squares	Df	Mean square	F -value	P value	Confidence level	Coefficient estimate	Standard error	95% CI low	95% CI high	Rank (%)
Model		16.77	14	1.20	47.71	<0.0001	99.99					
Linear effects	X_1 (initial pH level)	11.78	1	11.78	469.25	<0.0001	99.99	0.70	0.03	0.63	0.77	32.492
	X_2 (temperature)	0.02	1	0.02	0.72	0.4107	58.93	0.03	0.03	-0.04	0.10	1.269
	X_3 (incubation time)	1.62	1	1.62	64.44	<0.0001	99.99	0.26	0.03	0.19	0.33	12.040
	X_4 (plant extract volume)	0.13	1	0.13	5.30	0.0361	96.39	-0.07	0.03	-0.14	-0.01	3.453
Interaction effects	$X_1 X_2$	0.01	1	0.01	0.27	0.6114	38.86	-0.02	0.04	-0.10	0.06	0.953
	$X_1 X_3$	0.76	1	0.76	30.13	<0.0001	99.99	0.22	0.04	0.13	0.30	10.084
	$X_1 X_4$	0.01	1	0.01	0.46	0.5067	49.33	-0.03	0.04	-0.11	0.06	1.250
	$X_2 X_3$	0.35	1	0.35	13.78	0.0021	99.79	-0.15	0.04	-0.23	-0.06	6.820
	$X_2 X_4$	0.62	1	0.62	24.72	0.0002	99.98	-0.20	0.04	-0.28	-0.11	9.133
	$X_3 X_4$	0.34	1	0.34	13.57	0.0022	99.78	-0.15	0.04	-0.23	-0.06	6.768
Quadratic effects	X_1^2	0.05	1	0.05	1.94	0.1840	81.60	0.04	0.03	-0.02	0.11	1.954
	X_2^2	0.39	1	0.39	15.60	0.0013	99.87	-0.12	0.03	-0.18	-0.06	5.541
	X_3^2	0.05	1	0.05	1.80	0.1992	80.08	0.04	0.03	-0.02	0.11	1.885
	X_4^2	0.52	1	0.52	20.55	0.0004	99.96	0.14	0.03	0.07	0.20	6.360
Error effects	Lack of fit	0.31	10	0.03	2.44	0.1684						
	Pure error	0.06	5	0.01								
Std. Dev.		0.16		R-squared		0.9780						
Mean		1.43		Adj R-squared		0.9575						
C.V. (%)		11.08		Pred R-squared		0.8896						
PRESS		1.89		Adeq precision		25.1233						

extract volume, and incubation time \times the plant extract volume were also significant with probability values of $P < 0.0001$, $P = 0.0021$, $P = 0.0002$, and $P = 0.0022$, respectively (Table 2).

The determination coefficient (R^2) values indicate the extent to which the experimental factors and their interactions may contribute for the observed response values' variability. The R^2 value is always in the range of 0 to 1. When the R^2 value is close to 1, the model is more robust and accurate in predicting the response [46]. In this case, an R^2 of 0.9780 suggested that 97.80% of the total data variance is attributable to the tested variables (Table 2). Additionally, the Adj R^2 and predicted R^2 values are 0.9575 and 0.8896. The model's significance was confirmed by the model's exceptionally high Adj R^2 value (Table 2). The predicted R^2 value is very close to the adjusted R^2 value. This demonstrated a high degree of consistency between predicted and actual values for AgNP biosynthesis. "Adeq Precision" is a signal-to-noise ratio meter. A ratio greater than four is preferred. A value of 25.1233 for "Adeq Precision" shows an adequate signal-to-noise ratio. Additionally, in Table 2, the value of PRESS is 1.89; standard deviation value is 0.16, and mean value is 1.43 and a very low value of C.V.

(11.08) showing that this experimental performance was accurate and fit.

Table 3 summarizes the fit summary results obtained when linear, 2FI, and quadratic models were used to determine the optimal polynomial model for the experimental data on AgNP biosynthesis. The fit summary results indicated that the quadratic model of AgNP biosynthesis is highly significant, having an extremely low P value < 0.0001 . Lack of fit test for AgNP biosynthesis with F -value = 2.44 and P value = 0.1684 is nonsignificant. The model summary statistics for the quadratic model of AgNP biosynthesis (Table 3) revealed a low standard deviation of 0.16, a high adjusted R^2 of 0.9575, and a predicted R^2 of 0.8896.

2.3. Three-Dimensional Surface Plots. To show the factors' interactions and the optimal value of each variable required for maximum silver nanoparticle biosynthesis, three-dimensional response surface curves were generated to understand the factors' interaction effects. Each graph demonstrates the effect of two factors on the biosynthesis of AgNPs, with the other two variables remaining constant at their central value [44]. Figures 1(a)–1(f) depict the three-dimensional responses for the four variables by plotting

TABLE 3: Fit summary for experimental results of CCD for optimization of AgNP biosynthesis using *M. oleifera* leaf extract.

Model summary statistics					
Source	SD	R ²	Adjusted R ²	Predicted R ²	PRESS
Linear	0.38	0.7903	0.7568	0.6753	5.57
2FI	0.28	0.9118	0.8653	0.8073	3.30
Quadratic	0.16	0.9780	0.9575	0.8896	1.89
Lack of fit tests					
Source	SS	Df	MS	F-value	Pvalue
Linear	3.53	20	0.1765	13.78	0.0043
2FI	1.45	14	0.1035	8.08	0.0153
Quadratic	0.31	10	0.0313	2.44	0.1684
Pure error	0.06	5	0.0128		
Sequential model sum of squares					
Source	SS	Df	MS	F value	P value
Linear vs. mean	13.55	4	3.39	23.56	<0.0001
2FI vs. linear	2.08	6	0.35	4.36	0.0062
Quadratic vs. 2FI	1.14	4	0.28	11.31	0.0002
Residual	0.17	7	0.02		

MS: mean square; SS: sum of squares; SD: standard deviation; 2FI: two-factor interaction; PRESS: sum of squares of prediction error; Df: degree of freedom.

AgNP biosynthesis on the z -axis against pairs of process factors while keeping the value of the other two factors at their central value constant. They made it easier to understand the presence and magnitude of interdependencies between variables and to establish each parameter's optimum levels for maximum output of nanoparticle synthesis.

The three-dimensional plots in Figure 1(a) demonstrate that AgNP biosynthesis depended on the pH (X_1) and temperature (X_2) effects while the incubation time (X_3) and plant extract volume (X_4) were maintained at a zero level (8 h and 1.5 mL, respectively). Figure 1(b) shows a response surface plot for pH (X_1) against incubation time (X_3) while maintaining the temperature (X_2) and extract volume (X_4) at zero level (60°C and 1.5 mL, respectively). Figure 1(c) shows a response surface plot for the extract volume (X_4) and pH (X_1) while the incubation time (X_3) and temperature (X_2) were kept fixed at a zero level (8 hours and 60°C, respectively). Figure 1(d) shows a response surface plot for the incubation time (X_3) and temperature (X_2) while the pH (X_1) and extract volume (X_4) were kept fixed at a zero level (8.0 and 1.5 mL, respectively). Figure 1(e) shows a response surface plot for the extract volume (X_4) and temperature (X_2) while the incubation time (X_3) and the pH (X_1) were kept fixed at a zero level (8 h and 8.0, respectively). Figure 1(f) shows a response surface plot for the extract volume (X_4) and time (X_3) while the pH (X_1) and temperature (X_2) were kept fixed at a zero level (8.0 and 60°C, respectively). It was found from the plots that the maximum bio-

synthesis of AgNPs was achieved at a pH of 10, incubation temperature of 80°C for 10 hours, and a volume of extract of 1 mL.

The AgNP process mechanism is well known to depend on the temperature and pH because they may influence the AgNP net charge and functional group [47]. Mokgweetsi et al. investigated the optimum conditions for the biosynthesis of AgNPs using *M. oleifera* plant parts (flowers, leaves, and stem barks). They found the optimum conditions to be 40 min of reaction time at 85°C using leaves; the reaction time was increased to 60 min with flowers and stem barks [48].

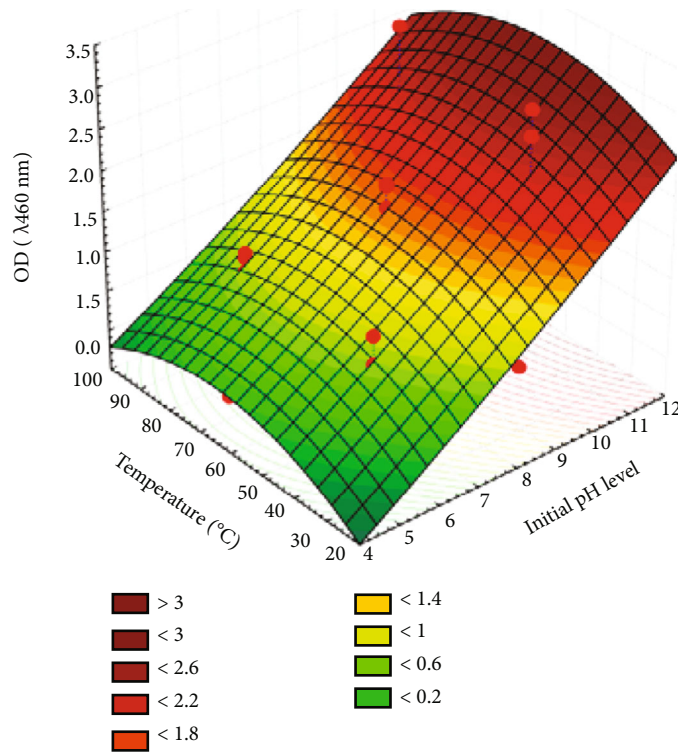
The particle size and morphological shape of the biologically synthesized NPs were affected by the pH, and the pH had a serious impact on the electrical charges of the capping agents and biomolecules, leading to a change in their ability to attach by reducing of metal ions [49]. Raising the temperature increases the production of AgNPs because new active adsorption sites form. Nevertheless, at temperatures above 50°C, metal biosorption can decrease owing to physical damage to the biosorbent surface or the destruction of certain active binding sites due to poor adaptive forces on the sites between the biosorbent surface and the metal ions [50].

2.4. Model Validation. The normal probability plot of the residuals is depicted in Figure 2(a). The residuals are regularly distributed and near to the diagonal line, showing that the model is well-fitting the data. It is essential to use the normal probability plot to determine whether the residuals have a normal distribution, in which case the points will follow a straight line [51]. The Box-Cox graph is depicted in Figure 2(b). Lambda's optimal value is within the maximum and minimum confidence ranges. There was no need for data transformations. The blue line is situated in the middle of the two red ones; this indicates that the model fits the experimental data well. The plot of predicted values vs. residuals of AgNP biosynthesis (Figure 2(c)) shows the residuals scattered uniformly and randomly parallel to the diagonal line, confirming the model's adequacy. Actual versus predicted silver nanoparticle biosynthesis is depicted in Figure 2(d). The presence of points close to the diagonal line indicates a significant correlation between the silver nanoparticle biosynthesis predicted by the model and the actual results.

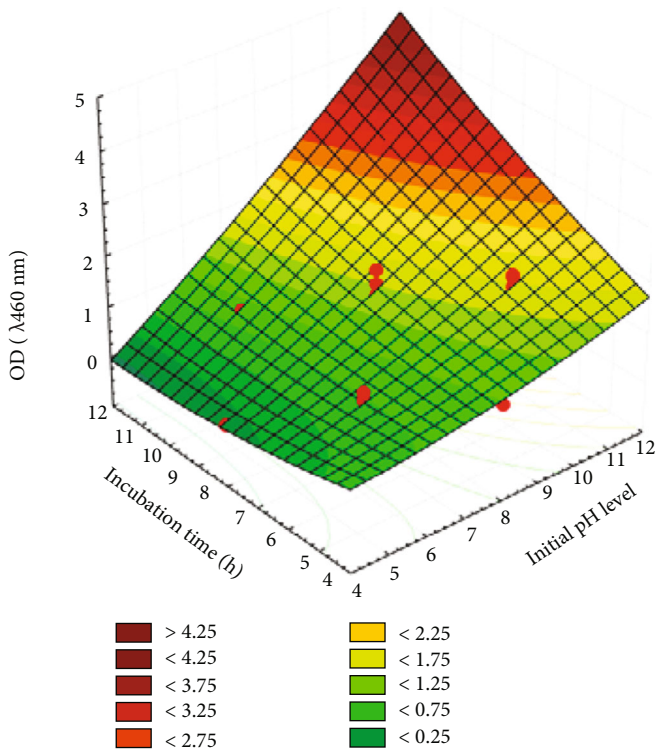
2.5. Characterization of Biosynthesized AgNPs

2.5.1. Color Change and UV-Vis Spectroscopy. Biofabrication of AgNPs can be confirmed using the chromatic shift of the substratum reaction as a visual marker. Nanometals display conspicuous spectral characteristics by surface plasmon resonance (SPR) based on the mutual vibration of free electrons and light wave resonance affected by the sizes and shapes of each of the synthesized NPs. This property is controlled by physical properties such as the form of the particles as to the size and shape and the local chemical effect [52, 53].

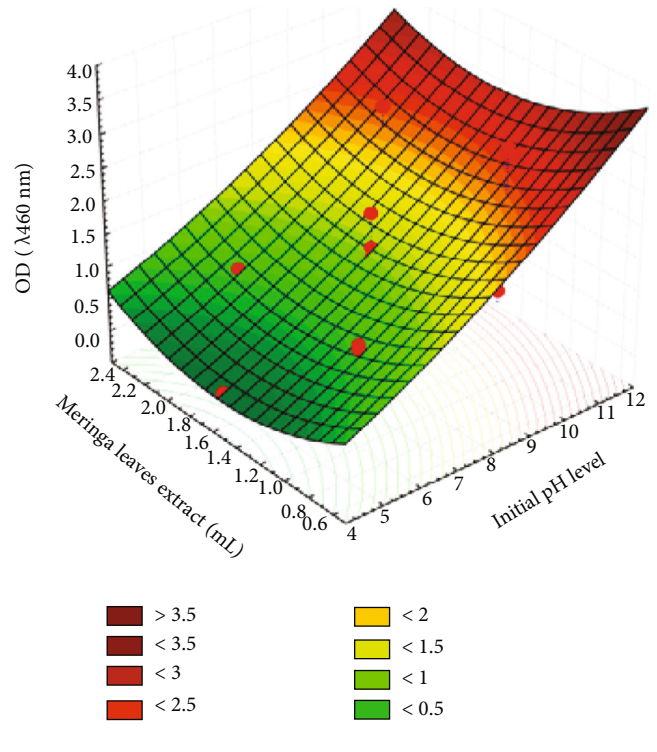
Figure 3 shows the development of 450 nm-based SPR AgNPs. This is in line with the findings of Bonigala et al. [54], who reported that the SPR zone of AgNPs appeared



(a)



(b)



(c)

FIGURE 1: Continued.

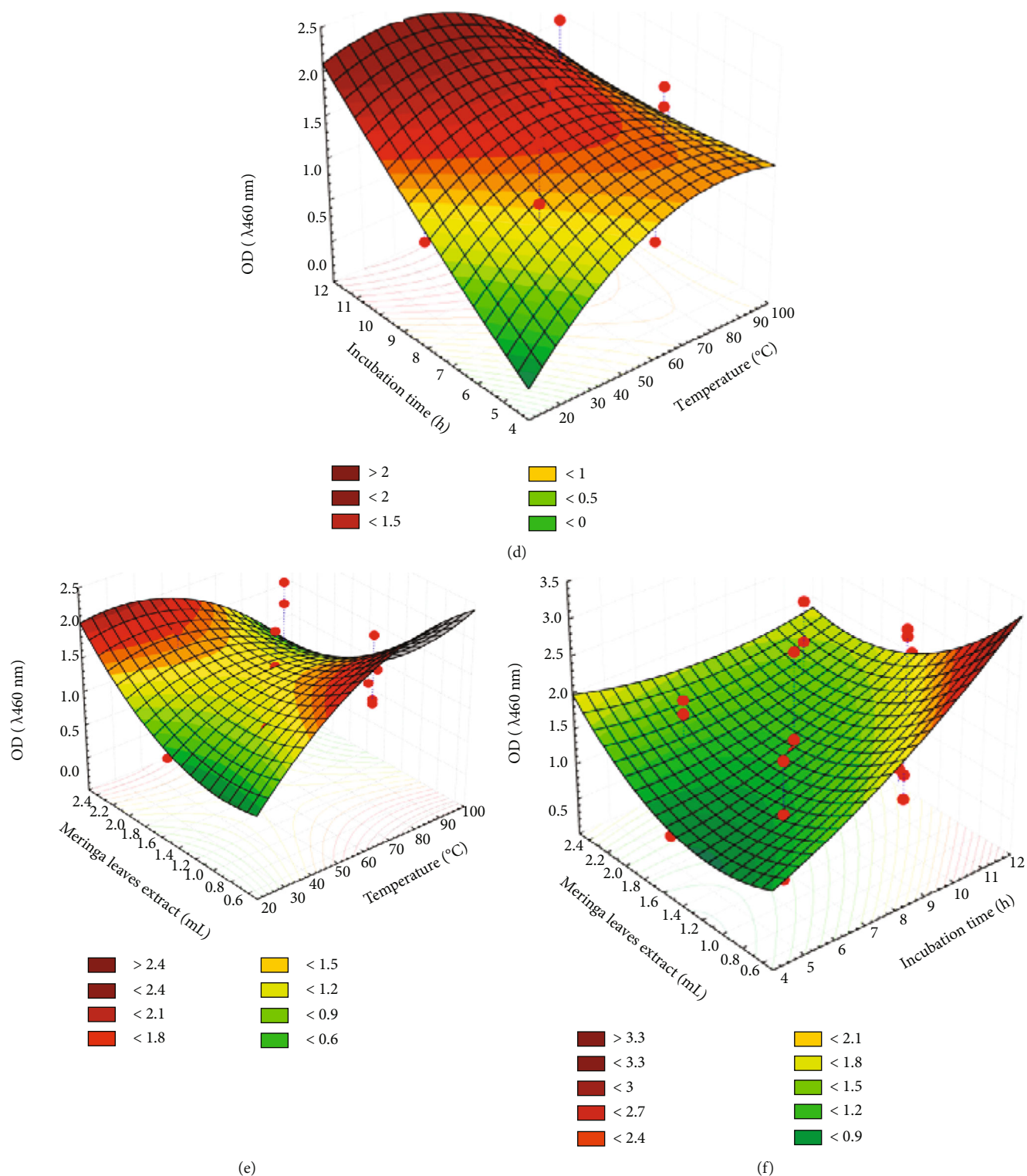


FIGURE 1: Three-dimensional plots showing the mutual effects of selected variables on AgNP biosynthesis with *M. oleifera* leaf extract.

exclusively within the range of \sim 400 to 500 nm. The change in color from yellow to brown suggested that the Ag^+ ion had been biotransformed into Ag^0 , becoming an AgNP [24]. The color shift in metal NPs was caused by surface plasmon vibration excitation [55].

On the contrary, the adsorption peak of the SPR of AgNPs was reported at different locations at 415 to 426 nm [48], 430 to 440 nm [24], and 440 to 450 nm [25] from leaf extracts of *M. oleifera* in different conditions.

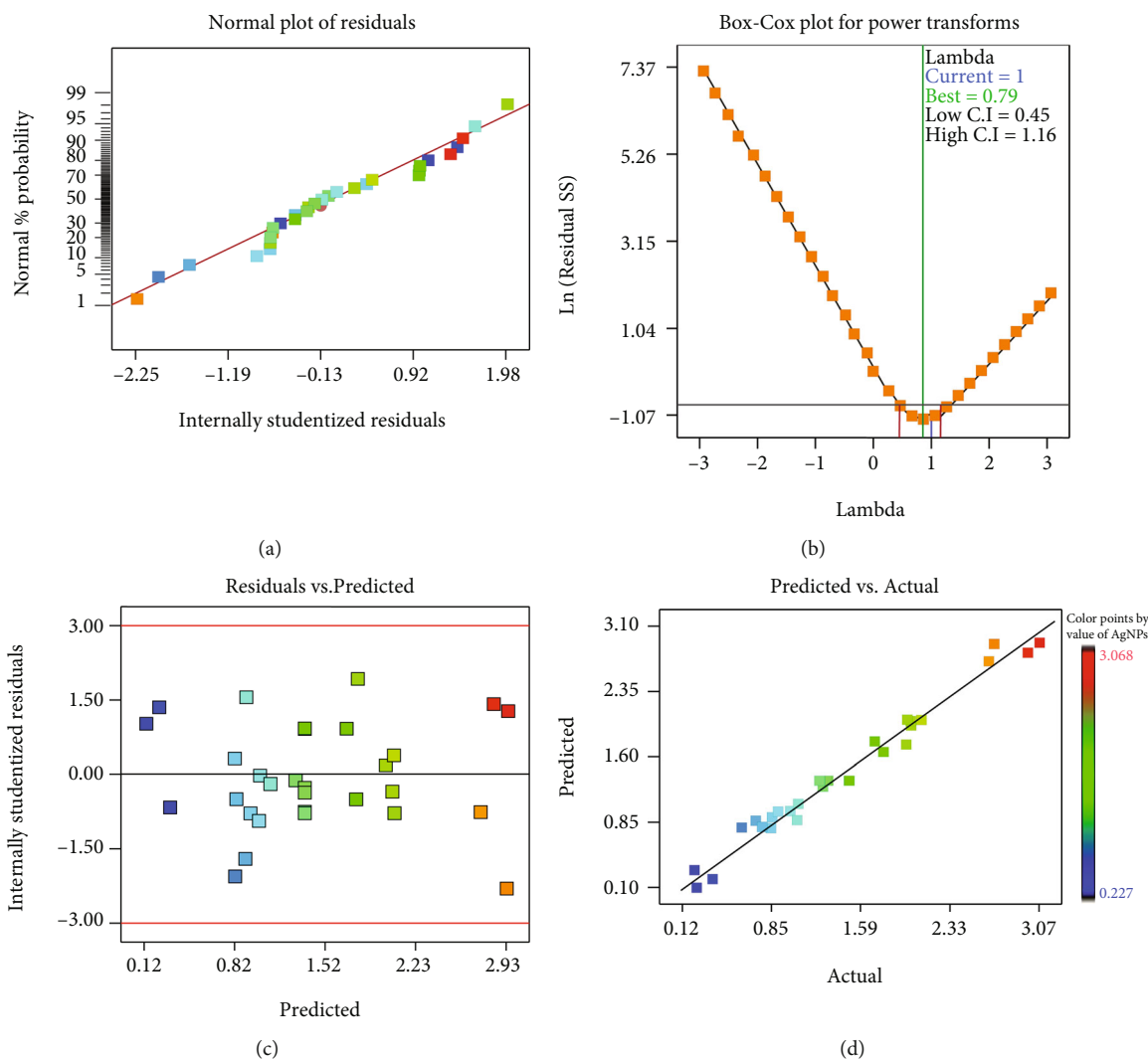


FIGURE 2: (a) Normal probability plot of internally studentized residuals, (b) Box-Cox plot of model transformation, (c) plot of internally studentized residuals versus predicted values, and (d) plot of predicted versus actual of AgNP biosynthesis by using *M. oleifera* leaf extract as determined by second-order polynomial equation.

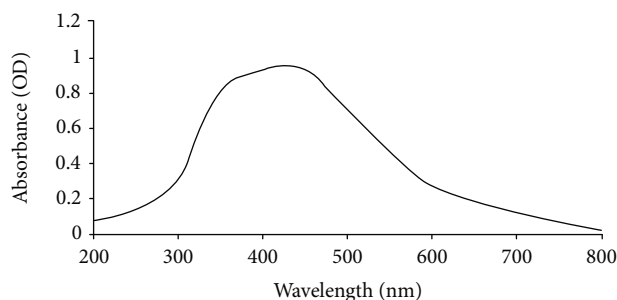


FIGURE 3: UV-visible spectrum recorded as a function of reaction time for an aqueous solution of 10^{-3} M AgNO_3 and *Moringa oleifera* leaf extract.

2.5.2. Transmission Electron Microscopy Imaging. Transmission electron microscopy (TEM) can provide details about the bulk content from a very low to a higher magnification [56]. TEM images demonstrated clearly that particles had a

spherical shape and that their sizes ranged from 15.22 to 29.45 nm (Figure 4). Furthermore, the biosynthesized NPs were distributed uniformly without morphological abnormalities or aggregation [57]. The biofunctional components

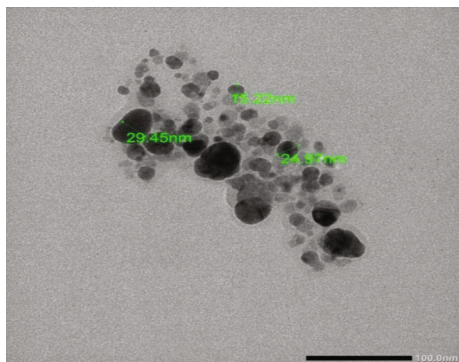


FIGURE 4: TEM image of AgNPs biosynthesized with *M. oleifera* leaf extract.

derived from nature (alkaloids, terpenes, fatty acids, and amino acids) were effective as stabilizing agents for preventing NP aggregation [58]. TEM imaging confirmed the green synthesis of AgNPs by *M. oleifera* aqueous extract [25]. A similar observation was made by Ghosh *et al.* [26], Prasad and Elumalai [24], and Moodley *et al.* [25] that the synthesized AgNPs had a spherical shape when using *M. oleifera* leaf extracts. Rodríguez- Félix *et al.* synthesized the AgNPs using safflower with the same characteristics (spherical shape, crystalline structure) [59]. Bapat *et al.* reported that the bioactivity of AgNPs depends on the morphological, charges, and surface properties of the AgNPs, in addition to the synergistic effects of AgNPs and cellular response and pH [60].

2.5.3. Fourier-Transform Infrared Spectroscopy Studies. Fourier-transform infrared (FTIR) spectroscopy studies of AgNPs were made to find out the possible compounds responsible for the efficient stabilization and capping of AgNPs synthesized with *M. oleifera* extract [61]. The FTIR spectra of stabilized AgNPs are shown in Figure 5. The spectral analysis found that the functional groups were responsible for reducing and stabilizing AgNPs while they were converted to their oxidized derivatives.

The stretching vibrations of the O–H functional groups in the structure (phenolic, alcoholic, and/or carboxylic acid compounds), as well as amine groups that might be overlapped with the O–H peak, were correlated to the broadband visible at 3000 to 3500 cm^{-1} [25, 31]. The infrared (IR) bands at 1631 to 1650 cm^{-1} were stretch vibrations of $\text{C}=\text{O}$ belonging to the amide II band (mainly from in-plane N–H bending), which is one of the major bands in the IR spectra of proteins. In fact, the peak at 1631 to 1650 cm^{-1} attributed to both $\text{C}=\text{C}$ stretching and amide (N–H) stretching could be involved in the protein stabilization of NPs [25, 31, 62]. The peak at 2000 to 2100 cm^{-1} was attributed to C–H bending in aromatic compounds such as flavonoids that existed in *M. oleifera* extract [20, 27]. The broadband at 680 to 500 cm^{-1} attributed to the aliphatic chain's bending region existed in the extract compounds [47]. A similar interpretation was reported by Mehwish *et al.* [31], Moodley *et al.* [25], and Bindhu *et al.* [27], who showed functional groups with slight peak shifts were presented in AgNPs, and this indicated the

reduction and stabilization of AgNPs by the extract of the *M. oleifera* leaf.

Infrared data indicated that the protein in the extract of *M. oleifera* was involved in the coating and biosynthesis of AgNPs [62]. The protein covering AgNPs prevents agglomeration [63]. According to reports, free amide groups in the protein molecules can interact with AgNPs [64]. The groups of carbonyl and free amine in the protein residues have a stronger potential to bind AgNPs to prevent the agglomeration and stabilization of AgNPs [65].

2.6. X-Ray Diffraction (XRD). The crystallinity of green synthesized AgNP-based leaf extract of *Moringa oleifera* was confirmed by the XRD (Figure 6). The XRD diffractogram at 2θ values identified the main integrated peaks at 27.79° , 32.08° , 45.88° , 56.88° , and 66.50° ; these bands were similar to the reported findings in a previous investigation on the crystalline nature of AgNPs [66].

2.7. Antimicrobial Activity of AgNPs. AgNP biosynthesized by the *M. oleifera* extract were investigated for antimicrobial effectiveness against various strains of pathogenic bacteria (*E. coli*, *K. pneumoniae*, *S. aureus*, and *B. subtilis*). The results reported in Table 4 show that AgNPs exhibited a zone of inhibition for all test species, either the Gram-negative (G-) strain (*E. coli* and *K. pneumoniae*) or Gram-positive (G+) strain (*S. aureus* and *B. subtilis*). The Gram-negative strain (*E. coli* and *K. pneumoniae*) is the most resistant bacterial species against the AgNPs synthesized in the current study (Figure 7). It displayed the smallest inhibition zone (17 and 11 mm, respectively) and the highest minimum inhibitory concentration (MIC) (3.6 and $5.8\text{ }\mu\text{g/mL}$, respectively). However, *S. aureus* was the most prone, with a maximum inhibition zone of 19 mm and the lowest MIC of $2.9\text{ }\mu\text{g/mL}$. The high sensitivity of (G+) bacteria may be attributed to the relative permeability of the outer membrane in contrast to (G-) bacteria [67]. Several mechanisms for understanding the antimicrobial activity of biosynthesized AgNPs have been postulated. Feng *et al.* [68] reported that AgNP antibacterial activity of Ag^+ ions is attributed to their ability to bind to various elements of bacterial cells, such as the cytoplasm and DNA molecules, which flow out of a wounded cell wall. The bacterial inactivation process of AgNPs can be caused by the peroxidation of membrane lipids and protein inactivation in the plasma membrane and cell wall, which weaken the structural integrity of the membrane, resulting in transport disorders and potassium leakage [69]. Similar findings were reported by Bindhu *et al.* [27], Prasad and Elumalai [24], and Ghosh *et al.* [26], who investigated the antimicrobial activity of AgNPs synthesized by the extract of *M. oleifera* against different pathogenic bacteria such as *Pseudomonas aeruginosa*, *Salmonella paratyphi*, *B. subtilis*, *K. pneumoniae*, and *E. coli*. They found that the most resistant strains were Gram-negative strains, especially *K. pneumoniae*, of the tested strains.

In the bacteria cell, AgNPs can interact with the signaling pathway during bacterial growth by regulating tyrosine phosphorylation on the substrates of the polypeptide that are important for cell proliferation [70]. Sondi and

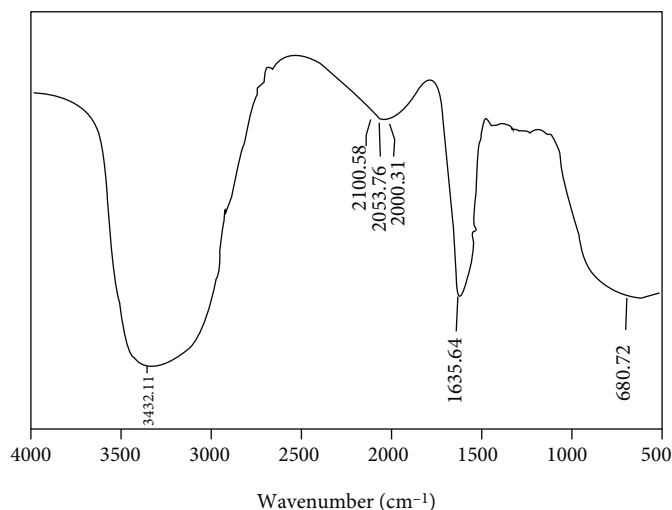


FIGURE 5: FTIR spectrum of aqueous extract of AgNPs synthesized with *M. oleifera* leaf extract.

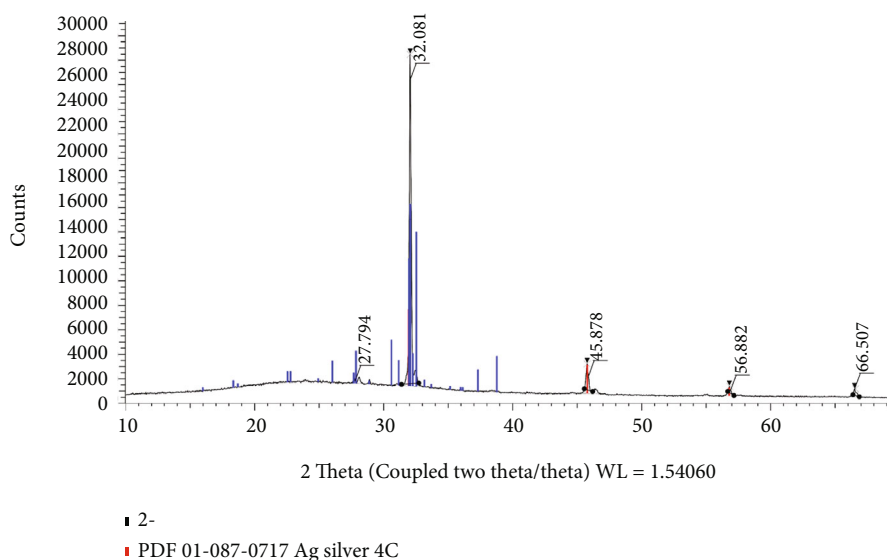


FIGURE 6: XRD diffractogram of AgNPs synthesized with *M. oleifera* leaf extract.

TABLE 4: Antibacterial activity of biosynthesized AgNPs from *M. oleifera* extract against bacterial pathogen strains.

Microorganism	ZOI* (mm)	MIC** ($\mu\text{g mL}^{-1}$)
<i>Escherichia coli</i>	17 \pm 0.3	3.6 \pm 0.034
<i>Klebsiella pneumonia</i>	11 \pm 0.2	5.8 \pm 0.023
<i>Staphylococcus aureus</i>	19 \pm 0.6	2.9 \pm 0.05
<i>Bacillus subtilis</i>	15 \pm 0.5	4 \pm 0.03

*ZOI: zone of inhibition diameter (mm); **MIC: minimal inhibitory concentrations ($\mu\text{g mL}^{-1}$).

Salopek-Sondi investigated the mechanism of AgNP penetration into *E. coli* and found that AgNPs led to the formation of pits in the plasma membrane that could be responsible for major increases in the permeability of the cell membrane, affecting transport through the cell membrane [71].

Furthermore, metal-induced free radicals such as reactive oxygen species (ROS) cause oxidative stress which can harm DNA, mitochondria, and bacterial membranes. The cell finally dies as a result of this [72]. Another possible effect of antibacterial activity by AgNPs is due to losing the ability for DNA replication and cellular synthesis of proteins after Ag^+ treatment [68]. Bindhu et al. [27], Prasad et al. [24], Moodley et al. [25], and Ghosh et al. [26] investigated the antimicrobial effect of AgNPs using *M. oleifera* extract. The combination of the antibacterial properties of AgNPs and *M. oleifera* produced an excellent antimicrobial agent against pathogenic microorganisms such as (*K. pneumoniae*, *S. aureus*, *E. coli*, *P. aeruginosa*, and *Candida albicans*).

2.8. Antioxidant Activity of AgNPs. The antioxidant potential of biosynthesized AgNPs is due to their high phenolic content, which was calculated by the DPPH radical scavenging assay [73]. The DPPH radical was scavenged by *M. oleifera*

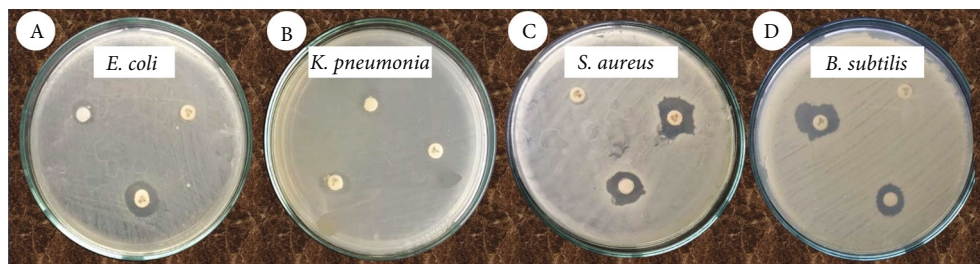


FIGURE 7: Effect of biosynthesized AgNPs from *M. oleifera* extract against bacterial pathogen strains.

TABLE 5: Radical scavenging activity of AgNPs synthesized with *M. oleifera* leaf extracts at different concentrations.

Concentration of plant extract (mg/mL)	% inhibition
4	11.96 ± 0.05
8	6.98 ± 0.03
12	16.95 ± 0.05
16	31.89 ± 0.1
20	63.79 ± 0.09

extracts in a dose-dependent technique (Table 5). The scavenging potency was increased if the concentration of *M. oleifera* extracts was increased. Based on statistical analysis, the highest percentage of scavenging (63.79%) was discovered at concentrations of 20 mg/mL, followed by concentrations of 16 mg/mL (31.89%) and 12 mg/mL (16.95%) ($P < 0.05$), whereas a concentration of 4 mg/mL showed the lowest scavenging capacity with a median value of 11.96% ($P < 0.05$).

Capped AgNPs were proved to have potent free radical scavenger activity. Antioxidants prevent oxidation by neutralizing the production of free radicals. The antioxidant activity of capped AgNPs is possibly due to the natural phytochemicals in the *M. oleifera* extract, which neutralize the free radicals produced [74]. It could also be due to the functional groups on the surface of AgNPs [75]. Some studies reported that the phenolic compounds in plant extracts are the main response for the antioxidant and antimicrobial activity of the NPs [76, 77].

3. Materials and Methods

3.1. Moringa Oleifera Plant Collection and Preparation of Leaf Extract. Fresh *M. oleifera* leaves were gathered from the local market in Giza, Egypt; cleaned in distilled water; and air-dried. The leaf material was kept in a freeze dryer for 72 h to remove all moisture and then stored at -16°C until use. Extrication processes were prepared by homogenization of 10 g of an *M. oleifera* leaf in 50 mL of distilled water, and the final volume was set at 100 mL. The flasks were coated with foil and incubated at 25°C for 24 h with shaking at 150 rpm. Then, the extracts were filtered by Whatman No. 1 filter paper (Whatman International Ltd, Maidstone, England).

3.2. Synthesis of AgNPs. Five mL extracts of *M. oleifera* leaves were added subsequently to 50 mL of the aqueous solution of AgNO_3 (1.0 mM). The suspension was stirred for 20 min with a magnetic stirrer and held at 25°C for 48 h in dark. The color changed from light brown to dark brown, which indicated the end of the reaction. The nanoparticles were recovered after synthesis by centrifugation at 15,000 rpm for 15 minutes, rinsed thoroughly with sterile distilled water, and dried overnight. The characterization tests and analysis were performed on this dry sample. A 50 mL aliquot containing 5 mL of distilled water was treated and utilized as a negative control in the experiments [11]. All experiments and analyses were performed in triplicate.

3.3. Biosynthesis Optimization of AgNPs via the Central Composite Design Matrix. The design matrix of central composite (CCD) is a surface-response technique used to evaluate the optimum rates of the major independent variables for increasing the AgNP biosynthesis. In the central composite model, four factors with the highest degrees of confidence were identified for further optimization (Table 1). These factors were pH (X_1 , 6–10), temperature (X_2 , 20– 80°C), incubation time (X_3), and plant extract volume (X_4), all experimental factors were evaluated in the absence of light and are presented in Table 1.

The central composite design matrix was created with 30 separate tests and 3 center points using Design-Expert software (Ver. 7). The significant variables were evaluated and coded at 3 levels (-1, 0, and +1) for the levels of low, middle, and high, respectively. To define and compare the relation between the AgNP biosynthesis (Y) and the relevant four factors, as well as to predict the optimal factor rates, the equation for polynomial was as follows:

$$Y = \beta_0 + \sum_i \beta_i X_i + \beta \sum_{(ii)} \beta_{(ii)} X_{ii} + \sum_{ij} \beta_{ij} X_i X_j, \quad (1)$$

where the code of Y is AgNP biosynthesis, β_0 is the regression coefficients, β_i is the linear coefficient, X_i is the independent variable rates, β_{ii} is the quadratic coefficients, and β_{ij} is the interaction coefficients. Trials were conducted in three replicates, with reported intermediate results.

3.4. Characterization and Analysis of AgNPs. The characterization and analysis of the biosynthesis of AgNPs were analyzed using a spectrophotometer (UV-Vis Vision Technology V3.20, ATI Unicam-5625) within 200–900 nm at the Faculty of Science, Mansoura University, Egypt. The

biofunctional groups of *Moringa oleifera* extract involved in the bioreduction of silver nanoparticles were determined by a Fourier transform infrared (FT-IR) (Thermo-Fisher Nicolet IS10, USA) in the region of 4000–500 cm^{-1} at a resolution of 1 cm^{-1} . The transmission of electron microscopy (TEM) (JEOL JSM-6510/v, Japan) was applied to characterize the morphological shape and particle size of the biosynthesized AgNPs. The crystallinity nature of biosynthesized AgNPs was studied using a D8-Advance X-ray diffractometer (Bruker, Germany); the analysis was performed at 40 kv, mA, scanning rate at 6°/min, and Cu $K\alpha$ radiation; the 2θ scanning ranged between 20 and 80° at 0.02 step size.

3.5. Microorganism. The experiments employed four normal microbial strains: *Escherichia coli* (ATCC-35218), *Klebsiella pneumoniae* (ATCC-700603), *Staphylococcus aureus* (ATCC-25923), and *Bacillus subtilis* (ATCC-27853). The bacterial cultures were cultivated and tested in media (Difco, Sparks, MD) for soy broth trypticase (TSB) and soy agar trypticase (TSA).

3.6. Paper Disc Diffusion Assay. Cell suspension (100 μL) was evenly distributed on TSA for disk diffusion assay. The inoculated agar was examined with impregnated discs of filter paper (Whatman No. 41, 6 mm diameter) with 25 μL plant extract at a concentration of 10 mg/mL. The antibacterial control agent was chloramphenicol/ketoconazole at a dosage of 10 mg/mL. Incubation of inoculated plate was incubated at 37°C/24 h. The diameter zone of the inhibition (ZOI) was then correctly determined, and the mean of their triplicates was estimated [78].

3.7. Determination of Minimal Inhibitory Concentration (MIC). To assess minimum inhibitory concentrations (MIC), each of the *Moringa oleifera* extracts was tested against examined bacterial strains as a quantitative assay [79]. As the predictor of bacterial production, *p*-iodonitro-tetrazolium violet (INT) was used in the method of broth's microdilution. Serial concentrations of *Moringa oleifera* extracts (50 μL of each well) were distributed on the plates of TSA and incubated for 24 h/37°C.

3.8. Antioxidant Activity of Silver Nanoparticles. The antioxidant activity of AgNPs was assayed using 2,2-diphenyl-1-picrylhydrazyl (DPPH) to determine the scavenging function of free radicals [80]. In this assay, the removal of the H-atom from the antioxidant compound leads to reducing the color of DPPH from violet to a pale-yellow. The assay reaction mixture contained 1 mL of AgNPs at various concentrations (10, 20, 30, 40, and 50 mg/mL) and 1 mL methanolic solution (0.1 mM) of DPPH and incubated under extreme shaking at 37°C for 0.5 hours. The absorbance of the mixture was measured at 517 nm, and the positive control was ascorbic acid. The higher scavenging activity of free radical was related to more decrease in absorbance, which was calculated using the following formula:

$$\text{DPPH scavenging activity (\%)} = \frac{100 \times (A_0 - A_1)}{A_0}, \quad (2)$$

where A_0 is the absorbances of the control and A_1 is the sample absorbances. The results are presented as the average of three replicate analyses, with the main values as well as the standard deviation (SD) provided.

3.9. Statistic Data Analysis. The design of the experiments and statistical analysis was done using Design-Expert software (Ver.7), and the 3D surface plots were drawn using Statistica® 8.0 (StatSoft Inc., Tulsa, USA).

4. Conclusion

The findings of this study suggest that AgNPs can be biofabricated from an aqueous extract of *M. oleifera*. The leaves of *M. oleifera* showed potent antioxidant and antibacterial activities. *M. oleifera* showed good potential for synthesizing AgNPs through rapid reduction of Ag^+ ions. The synthesized AgNPs had a spherical shape and high efficiency against some pathogenic microorganisms. They have potential uses as antioxidants for medical applications. A recommended approach for biosynthesis is using a green procedure for the biosynthesis of AgNPs because of their eco-friendly nature.

Data Availability

The data are ready when requested.

Conflicts of Interest

The authors have not declared any conflict of interests.

Authors' Contributions

A.B.A.M., A.M., H.M., and A.S.A. were responsible for the conceptualization. A.B.A.M., A.M., H.M., G.M.N., A.A., R.H.A., and A.S.A. were responsible for the methodology. A.M., M.S.A.E., S.S., D.H.A., W.N.H., and A.E. were responsible for the software. A.B.A.M., G.M.N., M.S.A.E., A.E., D.H.A., W.N.H., and R.H.A. were responsible for the validation. A.B.A.M., A.M., H.M., M.S.A.E., R.H.A., A.A., D.H.A., W.N.H., and A.S.A. were responsible for the formal analysis. A.B.A.M., A.M., H.M., G.M.N., A.A., R.H.A., and A.S.A. were responsible for the investigation. S.L. was responsible for resources. A.B.A.M., A.M., H.M., A.A., and A.E. were responsible for data curation. H.M., S.I., A.E., and A.A. were responsible for writing original draft preparation. A.A., R.H.A., and A.S.A. were responsible for writing, review, and editing. A.B.A.M., S.I., and A.S.A. were responsible for the visualization. A.B.A.M., H.M., and A.S.A. were responsible for the supervision. A.B.A.M., D.H.A., and A.S.A. were responsible for the funding acquisition. N.E.E. was responsible for experimental instructions, performed the statistical analysis, and prepared the figures and tables related to the optimization of AgNP biosynthesis. All authors have read and agreed to the published version of the manuscript. S.S and A.E in : validation, investigation, resources, funding and writing review and editing.

Acknowledgments

We thank Princess Nourah bint Abdulrahman University Researchers Supporting Project number PNURSP2022R15, Princess Nourah bint Abdulrahman University, Riyadh, Saudi Arabia; the University of Sadat City, Egypt; City of Scientific Research and Technological Applications-Egypt; and Cairo University, Egypt.

References

- [1] T. Hyeon, "Chemical synthesis of magnetic nanoparticles," *Chemical Communications*, vol. 8, pp. 927–934, 2003.
- [2] P. Mohanpuria, N. K. Rana, and S. K. Yadav, "Biosynthesis of nanoparticles: technological concepts and future applications," *Journal of Nanoparticle Research*, vol. 10, no. 3, pp. 507–517, 2008.
- [3] C. Jayaseelan, A. A. Rahuman, A. V. Kirthi et al., "Novel microbial route to synthesize ZnO nanoparticles using *Aeromonas hydrophila* and their activity against pathogenic bacteria and fungi," *Spectrochimica Acta Part A: Molecular and Biomolecular Spectroscopy*, vol. 90, pp. 78–84, 2012.
- [4] K. Gopinath, V. Karthika, S. Gowri, V. Senthilkumar, S. Kumaresan, and A. Arumugam, "Antibacterial activity of ruthenium nanoparticles synthesized using *Gloriosa superba* L. leaf extract," *Journal of Nanostructure in Chemistry*, vol. 4, no. 1, pp. 1–6, 2014.
- [5] A. K. Mittal, Y. Chisti, and U. C. Banerjee, "Synthesis of metallic nanoparticles using plant extracts," *Biotechnology Advances*, vol. 31, no. 2, pp. 346–356, 2013.
- [6] R. K. Das, V. L. Pachapur, L. Lonappan et al., "Biological synthesis of metallic nanoparticles: plants, animals and microbial aspects," *Nanotechnology for Environmental Engineering*, vol. 2, no. 1, pp. 1–21, 2017.
- [7] D. Bhattacharya and R. K. Gupta, "Nanotechnology and potential of microorganisms," *Critical Reviews in Biotechnology*, vol. 25, no. 4, pp. 199–204, 2005.
- [8] M. Soliman, S. H. Qari, A. Abu-Elsaoud, M. El-Esawi, H. Alhaithloul, and A. Elkelish, "Rapid green synthesis of silver nanoparticles from blue gum augment growth and performance of maize, fenugreek, and onion by modulating plants cellular antioxidant machinery and genes expression," *Acta Physiologiae Plantarum*, vol. 42, no. 9, p. 148, 2020.
- [9] K. B. Narayanan and N. Sakthivel, "Green synthesis of biogenic metal nanoparticles by terrestrial and aquatic phototrophic and heterotrophic eukaryotes and biocompatible agents," *Advances in Colloid and Interface Science*, vol. 169, no. 2, pp. 59–79, 2011.
- [10] I. Hussain, N. B. Singh, A. Singh, H. Singh, and S. C. Singh, "Green synthesis of nanoparticles and its potential application," *Biotechnology Letters*, vol. 38, no. 4, pp. 545–560, 2016.
- [11] P. Singh, Y. J. Kim, and D. C. Yang, "A strategic approach for rapid synthesis of gold and silver nanoparticles by *Panax ginseng* leaves," *Artificial Cells, Nanomedicine, and Biotechnology*, vol. 44, no. 8, pp. 1949–1957, 2016.
- [12] R. Navanietha Krishnaraj, "In vitro antiplatelet activity of silver nanoparticles synthesized using the microorganism *Glucobacter roseus*: an AFM-based study," *RSC Advances*, vol. 3, no. 23, pp. 8953–8959, 2013.
- [13] V. Castro-aceituno, S. Ahn, S. Yesmin, and P. Singh, "Anticancer activity of silver nanoparticles from *Panax ginseng* fresh leaves in human cancer cells," *Biomedicine & Pharmacotherapy*, vol. 84, pp. 158–165, 2016.
- [14] C. Rigo, L. Ferroni, I. Tocco et al., "Active silver nanoparticles for wound healing," *International Journal of Molecular Sciences*, vol. 14, no. 3, pp. 4817–4840, 2013.
- [15] K. Chaloupka, Y. Malam, and A. M. Seifalian, "Nanosilver as a new generation of nanoparticle in biomedical applications," *Trends in Biotechnology*, vol. 28, no. 11, pp. 580–588, 2010.
- [16] K. Vijayaraghavan, S. P. K. Nalini, N. U. Prakash, and D. Madhankumar, "One step green synthesis of silver nano/microparticles using extracts of *Trachyspermum ammi* and *Papaver somniferum*," *Colloids and Surfaces. B, Biointerfaces*, vol. 94, pp. 114–117, 2012.
- [17] K. Mohan Kumar, M. Sinha, B. K. Mandal, A. R. Ghosh, K. Siva Kumar, and P. Sreedhara Reddy, "Green synthesis of silver nanoparticles using *Terminalia chebula* extract at room temperature and their antimicrobial studies," *Spectrochimica Acta Part A: Molecular and Biomolecular Spectroscopy*, vol. 91, pp. 228–233, 2012.
- [18] E. J. Guidelli, A. P. Ramos, M. E. D. Zaniquelli, and O. Baffa, "Green synthesis of colloidal silver nanoparticles using natural rubber latex extracted from *Hevea brasiliensis*," *Spectrochimica Acta Part A: Molecular and Biomolecular Spectroscopy*, vol. 82, no. 1, pp. 140–145, 2011.
- [19] P. Tippayawat, N. Phromviyo, P. Boueroy, and A. Chompoosor, "Green synthesis of silver nanoparticles in aloe vera plant extract prepared by a hydrothermal method and their synergistic antibacterial activity," *PeerJ*, vol. 4, article e2589, 2016.
- [20] A. E. Mohammed, A. Al-Qahtani, A. Al-Mutairi, B. Al-Shamri, and K. Aabed, "Antibacterial and cytotoxic potential of biosynthesized silver nanoparticles by some plant extracts," *Nanomaterials*, vol. 8, no. 6, p. 382, 2018.
- [21] A. Leone, A. Spada, A. Battezzati, A. Schiraldi, J. Aristil, and S. Bertoli, "Cultivation, genetic, ethnopharmacology, phytochemistry and pharmacology of *Moringa oleifera* leaves: an overview," *International Journal of Molecular Sciences*, vol. 16, no. 12, pp. 12791–12835, 2015.
- [22] D. Sivakumar, L. Chen, and Y. Sultanbawa, "A comprehensive review on beneficial dietary phytochemicals in common traditional Southern African leafy vegetables," *Food Science & Nutrition*, vol. 6, no. 4, pp. 714–727, 2018.
- [23] C. K. Dalukdeniya and U. Rathnayaka, "Antimicrobial activity of different extracts of leaves bark and roots of *Moringa oleifera* (Lam)," *International Journal of Current Microbiology and Applied Sciences*, vol. 5, no. 7, pp. 687–691, 2016.
- [24] T. N. V. K. V. Prasad and E. K. Elumalai, "Biofabrication of Ag nanoparticles using *Moringa oleifera* leaf extract and their antimicrobial activity," *Asian Pacific Journal of Tropical Biomedicine*, vol. 1, no. 6, pp. 439–442, 2011.
- [25] J. S. Moodley, S. B. Krishna, K. Pillay, and P. Govender, "Green synthesis of silver nanoparticles from *Moringa oleifera* leaf extracts and its antimicrobial potential," *Advances in Natural Sciences: Nanoscience and Nanotechnology*, vol. 9, no. 1, article 015011, 2018.
- [26] A. Abdel-Azeem, A. A. Nada, A. O'Donovan, V. Kumar Thakur, and A. Elkelish, "Mycogenic silver nanoparticles from endophytic trichoderma atroviride with antimicrobial activity," *Journal of Renewable Materials*, vol. 7, no. 11, pp. 171–185, 2019.

- [27] M. R. Bindhu, M. Umadevi, G. A. Esmail, N. A. Al-Dhabi, and M. V. Arasu, "Green synthesis and characterization of silver nanoparticles from *Moringa oleifera* flower and assessment of antimicrobial and sensing properties," *Journal of Photochemistry and Photobiology B: Biology*, vol. 205, article 111836, 2020.
- [28] W. G. Shousha, W. M. Aboulthana, A. H. Salama, M. H. Saleh, and E. A. Essawy, "Evaluation of the biological activity of *Moringa oleifera* leaves extract after incorporating silver nanoparticles, *in vitro* study," *Bulletin of the National Research Centre*, vol. 43, no. 1, article 212, 2019.
- [29] M. Iqbal, N. I. Raja, M. Hussain et al., "Morphological fabrication of immobilized green synthesized silver nanoparticles," *Nanoscience and Nanotechnology Letters*, vol. 10, no. 11, pp. 1508–1514, 2018.
- [30] S. Das, U. K. Parida, and B. K. Bindhani, "Green biosynthesis of silver nanoparticles using *Moringa oleifera* L. leaf," *International Journal of Nanotechnology and Application*, vol. 3, pp. 51–62, 2013.
- [31] H. M. Mehwish, M. S. R. Rajoka, Y. Xiong et al., "Green synthesis of a silver nanoparticle using *Moringa oleifera* seed and its applications for antimicrobial and sun-light mediated photocatalytic water detoxification," *Journal of Environmental Chemical Engineering*, vol. 9, no. 4, article 105290, 2021.
- [32] G. Nilanjuna, P. Samrat, and B. Piyali, "Silver nanoparticles of *Moringa oleifera* – green synthesis, characterisation and its antimicrobial efficacy," *Journal of Drug Delivery and Therapeutics*, vol. 11, pp. 20–25, 2014.
- [33] A. A. Ezhilarasi, J. J. Vijaya, K. Kaviyarasu, M. Maaza, A. Ayeshamariam, and L. J. Kennedy, "Green synthesis of NiO nanoparticles using *Moringa oleifera* extract and their biomedical applications: cytotoxicity effect of nanoparticles against HT-29 cancer cells," *Journal of Photochemistry and Photobiology B: Biology*, vol. 164, pp. 352–360, 2016.
- [34] A. Islam, C. Mandal, and A. Habib, "Antibacterial potential of synthesized silver nanoparticles from leaf extract of *Moringa oleifera*," *Journal of Advanced Biotechnology and Experimental Therapeutics*, vol. 4, no. 1, pp. 67–73, 2021.
- [35] T. G. M. Mohammad and A. F. Abd El-Rahman, "Environmentally friendly synthesis of silver nanoparticles using *Moringa oleifera* (Lam) leaf extract and their antibacterial activity against some important pathogenic bacteria," *Mycopathologia*, vol. 13, pp. 1–6, 2015.
- [36] N. E.-A. El-Naggar, A. Mohamedin, S. S. Hamza, and A.-D. Sherief, "Extracellular biofabrication, characterization, and antimicrobial efficacy of silver nanoparticles loaded on cotton fabrics using newly isolated *Streptomyces* sp. SSHH-1E," *Journal of Nanomaterials*, vol. 2016, Article ID 3257359, 2016.
- [37] B. Ajitha, Y. A. K. Reddy, and P. S. Reddy, "Biogenic nanoscale silver particles by *Tephrosia purpurea* leaf extract and their inborn antimicrobial activity," *Spectrochimica Acta Part A: Molecular and Biomolecular Spectroscopy*, vol. 121, pp. 164–172, 2014.
- [38] B. Sadeghi and F. Gholamhoseinpoor, "A study on the stability and green synthesis of silver nanoparticles using *Ziziphora tenuior* (Zt) extract at room temperature," *Spectrochimica Acta Part A: Molecular and Biomolecular Spectroscopy*, vol. 134, pp. 310–315, 2015.
- [39] A. Shafaghat, "Synthesis and characterization of silver nanoparticles by phytosynthesis method and their biological activity," *Synthesis and Reactivity in Inorganic, Metal-Organic, and Nano-Metal Chemistry*, vol. 45, no. 3, pp. 381–387, 2015.
- [40] R. Veerasamy, T. Z. Xin, S. Gunasagaran et al., "Biosynthesis of silver nanoparticles using mangosteen leaf extract and evaluation of their antimicrobial activities," *Journal of Saudi Chemical Society*, vol. 15, no. 2, pp. 113–120, 2011.
- [41] R. Sarkar, P. Kumbhakar, and A. K. Mitra, "Green synthesis of silver nanoparticles and its optical properties," *Digest Journal of Nanomaterials and Biostructures*, vol. 5, pp. 491–496, 2010.
- [42] N. E.-A. El-Naggar, M. H. Hussein, and A. A. El-Sawah, "Phycobiliprotein-mediated synthesis of biogenic silver nanoparticles, characterization, *in vitro* and *in vivo* assessment of anticancer activities," *Scientific Reports*, vol. 8, no. 1, p. 8925, 2018.
- [43] N. E.-A. El-Naggar, N. A. M. Abdelwahed, and O. M. M. Darwesh, "Fabrication of biogenic antimicrobial silver nanoparticles by *Streptomyces aegyptia* NEAE 102 as eco-friendly nanofactory," *Journal of Microbiology and Biotechnology*, vol. 24, no. 4, pp. 453–464, 2014.
- [44] A. Mohamedin, N. E.-A. El-Naggar, S. Shawqi Hamza, and A. A. Sherief, "Green synthesis, characterization and antimicrobial activities of silver nanoparticles by *Streptomyces viridodiataticus* SSHH-1 as a living nanofactory: statistical optimization of process variables," *Current Nanoscience*, vol. 11, no. 5, pp. 640–654, 2015.
- [45] N. E.-A. El-Naggar, "Extracellular production of the oncolytic enzyme, L-asparaginase, by newly isolated *Streptomyces* sp. strain NEAE-95 as potential microbial cell factories: optimization of culture conditions using response surface methodology," *Current Pharmaceutical Biotechnology*, vol. 16, no. 2, pp. 162–178, 2015.
- [46] N. E.-A. El-Naggar and N. A. M. Abdelwahed, "Application of statistical experimental design for optimization of silver nanoparticles biosynthesis by a nanofactory *Streptomyces viridochromogenes*," *Journal of Microbiology*, vol. 52, no. 1, pp. 53–63, 2014.
- [47] R. A. Hamouda, M. H. Hussein, R. A. Abo-elmagd, and S. S. Bawazir, "Synthesis and biological characterization of silver nanoparticles derived from the cyanobacterium *Oscillatoria limnetica*," *Scientific Reports*, vol. 9, no. 1, article 13071, 2019.
- [48] P. Mokgweetsi, B. M. Bonang, and N. I. Chibua, "Green synthesis of silver nanoparticles using *Moringa oleifera*, employing multivariate optimization methodologies," *International Journal of Advanced Research*, vol. 6, no. 7, pp. 953–962, 2018.
- [49] M. Hasan, I. Ullah, H. Zul, K. Naeem, A. Iqbal, and H. Gul, "Biological entities as chemical reactors for synthesis of nanomaterials: progress, challenges and future perspective," *Materials Today Chemistry*, vol. 8, pp. 13–28, 2018.
- [50] N. E.-A. El-Naggar, R. A. Hamouda, I. E. Mousa, M. S. Abdel-Hamid, and N. H. Rabei, "Biosorption optimization, characterization, immobilization and application of *Gelidium amansii* biomass for complete Pb²⁺ removal from aqueous solutions," *Scientific Reports*, vol. 8, no. 1, article 13456, 2018.
- [51] N. E.-A. El-Naggar, M. H. Hussein, and A. A. El-Sawah, "Biofabrication of silver nanoparticles by phycocyanin, characterization, *in vitro* anticancer activity against breast cancer cell line and *in vivo* cytotoxicity," *Scientific Reports*, vol. 7, no. 1, article 10844, 2017.
- [52] M. Focsan, A. M. Gabudean, V. Canpean, D. Maniu, and S. Astilean, "Formation of size and shape tunable gold nanoparticles in solution by bio-assisted synthesis with bovine serum albumin in native and denaturated state," *Materials Chemistry and Physics*, vol. 129, no. 3, pp. 939–942, 2011.

- [53] R. A. Hamouda, A. I. Abd El Maksoud, M. Wageed et al., "Characterization and anticancer activity of biosynthesized Au/cellulose nanocomposite from *Chlorella vulgaris*," *Polymers*, vol. 13, no. 19, p. 3340, 2021.
- [54] B. Bonigala, K. M. Usha, M. Vijayalakshmi, R. Sambasiva, V. A. Ravi, and S. Poda, "Green synthesis of silver nanoparticles from leaf extract of *Cascabela thevetia*, physicochemical characterisation and antimicrobial activity," *Journal of Pharmacy Research*, vol. 10, pp. 410–418, 2016.
- [55] A. Ahmad, P. Mukherjee, S. Senapati, D. Mandal, M. I. Khan, and M. Sastry, "Extracellular biosynthesis of silver nanoparticles using the fungus *Fusarium oxysporum*," *Colloids and Surfaces B: Biointerfaces*, vol. 28, no. 4, pp. 313–318, 2003.
- [56] I. Khan, K. Saeed, and I. Khan, "Nanoparticles: properties, applications and toxicities," *Arabian Journal of Chemistry*, vol. 12, no. 7, pp. 908–931, 2019.
- [57] R. Sathyavathi, M. Krishna, and D. N. Rao, "Biosynthesis of silver nanoparticles using *Moringa oleifera* leaf extract and its application to optical limiting," *Journal of Nanoscience and Nanotechnology*, vol. 11, no. 3, pp. 2031–2035, 2011.
- [58] M. Plaza, S. Santoyo, L. Jaime, G. G. Reina, and E. Ibá, "Screening for bioactive compounds from algae," *Journal of Pharmaceutical and Biomedical Analysis*, vol. 51, no. 2, pp. 450–455, 2010.
- [59] F. Rodríguez-Félix, A. G. López-Cota, M. J. Moreno-Vásquez et al., "Sustainable-green synthesis of silver nanoparticles using safflower (*Carthamus tinctorius* L.) waste extract and its antibacterial activity," *Heliyon*, vol. 7, no. 4, article e06923, 2021.
- [60] M. S. Bapat, H. Singh, S. K. Shukla et al., "Evaluating green silver nanoparticles as prospective biopesticides: an environmental standpoint," *Chemosphere*, vol. 286, Part 2, article 131761, 2022.
- [61] F. Foroohimanjili, A. Mirzaie, S. M. M. Hamdi et al., "Antibacterial, antibiofilm, and quorum sensing activities of phyto-synthesized silver nanoparticles fabricated from *Mespilus germanica* extract against multidrug resistance of *Klebsiella pneumoniae* clinical strains," *Journal of Basic Microbiology*, vol. 60, no. 3, pp. 216–230, 2020.
- [62] M. L. Guimarães, F. A. G. da Silva, M. M. da Costa, and H. P. de Oliveira, "Green synthesis of silver nanoparticles using *Ziziphus joazeiro* leaf extract for production of antibacterial agents," *Applied Nanoscience*, vol. 10, no. 4, pp. 1073–1081, 2020.
- [63] R. Shanmuganathan, D. MubarakAli, D. Prabakar et al., "An enhancement of antimicrobial efficacy of biogenic and ceftriaxone-conjugated silver nanoparticles: green approach," *Environmental Science and Pollution Research*, vol. 25, no. 11, pp. 10362–10370, 2018.
- [64] S. Sarkar, A. D. Jana, S. K. Samanta, and G. Mostafa, "Facile synthesis of silver nano particles with highly efficient antimicrobial property," *Polyhedron*, vol. 26, no. 15, pp. 4419–4426, 2007.
- [65] R. Sangeetha, P. Niranjana, and N. Dhanalakshmi, "Characterization of silver nanoparticles synthesized using the extract of the leaves of *Tridax procumbens*," *Research Journal of Medicinal Plants*, vol. 10, no. 2, pp. 159–166, 2016.
- [66] M. Divya, G. S. Kiran, S. Hassan, and J. Selvin, "Biogenic synthesis and effect of silver nanoparticles (AgNPs) to combat catheter-related urinary tract infections," *Biocatalysis and Agricultural Biotechnology*, vol. 18, article 101037, 2019.
- [67] Z. Schelz, J. Molnar, and J. Hohmann, "Antimicrobial and antiplasmid activities of essential oils," *Fitoterapia*, vol. 77, no. 4, pp. 279–285, 2006.
- [68] Q. L. Feng, J. Wu, G. Q. Chen, F. Z. Cui, T. N. Kim, and J. O. Kim, "A mechanistic study of the antibacterial effect of silver ions on *Escherichia coli* and *Staphylococcus aureus*," *Journal of Biomedical Materials Research*, vol. 52, no. 4, pp. 662–668, 2000.
- [69] X.-H. N. Xu, W. J. Brownlow, S. V. Kyriacou, Q. Wan, and J. J. Viola, "Real-time probing of membrane transport in living microbial cells using single nanoparticle optics and living cell imaging," *Biochemistry*, vol. 43, no. 32, pp. 10400–10413, 2004.
- [70] V. Gopinath, S. Priyadarshini, M. F. Loke et al., "Biogenic synthesis, characterization of antibacterial silver nanoparticles and its cell cytotoxicity," *Arabian Journal of Chemistry*, vol. 10, no. 8, pp. 1107–1117, 2017.
- [71] I. Sondi and B. Salopek-Sondi, "Silver nanoparticles as antimicrobial agent: a case study on *E. coli* as a model for Gram-negative bacteria," *Journal of Colloid and Interface Science*, vol. 275, no. 1, pp. 177–182, 2004.
- [72] D. P. Tamboli and D. S. Lee, "Mechanistic antimicrobial approach of extracellularly synthesized silver nanoparticles against gram positive and gram negative bacteria," *Journal of Hazardous Materials*, vol. 260, pp. 878–884, 2013.
- [73] M. C. Foti, C. Biomolecolare, and P. Gaifami, "Use and abuse of the DPPH• radical," *Journal of Agricultural and Food Chemistry*, vol. 63, no. 40, pp. 8765–8776, 2015.
- [74] A. S. Shahat and N. H. Assar, "Biochemical and antimicrobial studies of biosynthesized silver nanoparticles using aqueous extract of *Myrtus communis* L.," *Annals of Biological Research*, vol. 6, pp. 10–90, 2015.
- [75] A. K. Keshari, R. Srivastava, P. Singh, V. B. Yadav, and G. Nath, "Antioxidant and antibacterial activity of silver nanoparticles synthesized by *Cestrum nocturnum*," *Journal of Ayurveda and Integrative Medicine*, vol. 11, no. 1, pp. 37–44, 2020.
- [76] C. L. Del-Toro-Sánchez, F. Rodríguez-Félix, F. J. Cinco-Moroyoqui et al., "Recovery of phytochemical from three safflower (*Carthamus tinctorius* L.) by-products: Antioxidant properties, protective effect of human erythrocytes and profile by UPLC-DAD-MS," *Journal of Food Processing & Preservation*, vol. 45, no. 9, article e15765, 2021.
- [77] K. Kanthi Gudimella, G. Gedda, P. S. Kumar et al., "Novel synthesis of fluorescent carbon dots from bio-based *Carica Papaya* leaves: optical and structural properties with antioxidant and anti-inflammatory activities," *Environmental Research*, vol. 204, no. Part A, article 111854, 2022.
- [78] M. Balouiri, M. Sadiki, and S. K. Ibsouda, "Methods for *in vitro* evaluating antimicrobial activity: a review," *Journal of Pharmaceutical Analysis*, vol. 6, no. 2, pp. 71–79, 2016.
- [79] A. A. Tayel, W. F. El-Tras, S. Moussa et al., "Antibacterial action of zinc oxide nanoparticles against foodborne pathogens," *Journal of Food Safety*, vol. 31, no. 2, pp. 211–218, 2011.
- [80] P. McCue, A. Horii, and K. Shetty, "Mobilization of phenolic antioxidants from defatted soybean powders by *Lentinus edodes* during solid-state bioprocessing¹ is associated with enhanced production of laccase," *Innovative Food Science and Emerging Technologies*, vol. 5, no. 3, pp. 385–392, 2004.